FULL-WAVE ATTENUATION RECONSTRUCTION IN THE TIME DOMAIN FOR ULTRASOUND COMPUTED TOMOGRAPHY

M. Pérez-Liva[1,2], J.L. Herraiz[1], J.M Udías[1], B.T. Cox[2], B.E. Treeby[2]

1. Grupo de Física Nuclear, Departamento de Física Atómica, Molecular y Nuclear, CEI Moncloa, Universidad Complutense de Madrid
2. Department of Medical Physics and Biomedical Engineering, University College London, Gower Street, London, WC1E 6BT, United Kingdom

ABSTRACT

Acoustical attenuation (AA) maps in Ultrasound Computed Tomography (USCT) provide enhanced contrast between tissues compared to the speed of sound (SS), which is the most common property of tissue studied with this technique. Currently, the full wave inversion (FWI) methods used for their reconstruction are very different: the AA is mainly estimated using frequency domain algorithms, while the SS is more often recovered in the time domain. In this work we present a novel strategy to recover the attenuation maps through a straightforward and simplified procedure in the time domain. A gradient descent method was employed to optimize iteratively the attenuation distribution. The expression for the functional gradient of the norm of the global deviation between experimental and simulated data was obtained using an adjoint method. The optimization code, implemented in C++, employs a CUDA version of the k-Wave software to perform forward and backward wave propagation. Noisy simulated data was used to test the performance of the proposed method. The simplicity of the formulation of this new method may facilitate the reconstruction of AA and SS maps under a common framework in USCT.

Index Terms— USCT, attenuation maps, full-wave inversion, adjoint method, gradient-descent.

1. INTRODUCTION

Ultrasound Computed Tomography (USCT) is a promising non-invasive and non-ionizing imaging modality that can be used to study the acoustical properties of tissues in the body. In this technique, the tissue is inspected through a set of ultrasound transducers which are located surrounding the region of interest. The transmitted and scattered pulses are registered in several angles and positions and later employed to recover the spatial distribution of properties like the SS or the AA, among others. The SS is well correlated with the tissue density and therefore, it can provide similar structural information to X-ray mammograms [1] (Fig. 1). Consequently, imaging the SS could provide an interesting alternative to detect breast cancer, avoiding the radiation and painful compression present in X-ray mammography. On the other hand, AA can provide enhanced contrast between different tissue types compared to the SS (Fig. 1) [1]. This may offer better discrimination of soft tissues, which could improve the detection of malignancies.

The reconstruction of the mentioned acoustic properties with FWI algorithms offers very high resolution and excellent image quality in general, because by solving the full wave equation (FWE) they account for all the main processes experienced by the wave [2-5]. Nevertheless, due to the computational burden of FWI methods (they require solving the FWE several times in each iterative step), the reconstruction of SS and AA has been generally treated with methods based on simplifications of the FWE (for example the commonly employed ray-tracing algorithm [6]). However, this affects the resolution of the reconstructed images. The reconstruction of SS with FWI has been widely studied in USCT, mainly extending geophysical reconstruction methods to this medical modality (generally neglecting the presence of AA and employing time-domain methodologies) [2, 3]. As a result, the potential of these methods to improve image quality has been demonstrated. However, the reconstruction of AA with FWI, despite being an extensively documented problem in seismology (generally treated in the frequency-domain), has been less studied for USCT than SS FWI-reconstructions. In the references [4, 5] a FWI formulation in the frequency-domain was introduced to obtain the quality factors (which indicates the energy loss per cycle) of the tissues to characterize the AA. The method employs a combination of several carefully-chosen sets of frequencies and therefore several minimization problems need to be performed. Moreover, as reference [7] demonstrates, fixed-frequency algorithms are hampered by instabilities and erroneous convergence at high frequencies evidencing the need for time-domain methods where the entire bandwidth of the signals can be employed.

As both acoustical properties (SS and AA) can be obtained from the same data, it is desirable to have a common framework in which both distributions can be recovered under a similar scheme, preferably using the image-quality

advantages provided by the FWI methods but at the same time enhancing its computational efficiency.

In this work we propose a novel strategy to recover the attenuation distribution (specifically we will obtain the distribution of the absorption coefficient), following a very straightforward and efficient scheme in the time domain, using the entire bandwidth of the signals. The proposed method is initiated with an estimate of the speed of sound distribution, which we assume has been obtained using standard FWI algorithms [2,3,13] totally compatible with the one proposed in this work to update the AA.

2. FORWARD MODEL

Consider a lossy medium in which the acoustic absorption follows a frequency power law:

$$\alpha = \alpha_0 \omega^y \tag{1}$$

where α_0 is the proportionality absorption coefficient in Np (rad/s)$^{-y}$ m^{-1}, ω is the temporal frequency, and y is the power law exponent which we assume to be constant and equal to 1.5 (the value given for breast tissue in [8]).

The changes produced in the medium by the propagating acoustic waves can be described by a series of coupled first-order partial differential equations based on the conservation of momentum, mass, and energy [9]:

$$\begin{aligned} \frac{d\boldsymbol{u}}{dt} &= -\frac{1}{\rho_0}\nabla p \\ \frac{d\rho}{dt} &= -\rho_0 \nabla \cdot \mathbf{u} - \mathbf{u} \cdot \nabla \rho_0 \\ p &= c_0^2(\rho + \boldsymbol{d} \cdot \nabla \rho_0 - L\rho) \end{aligned} \tag{2}$$

Here $\boldsymbol{d}$ is the acoustic particle displacement, $\mathbf{u}$ is the particle velocity, p is the pressure and ρ is the density of the medium. The operator L in the pressure-density relation is a linear integro-differential operator that accounts for acoustic absorption and dispersion.

$$L = \tau_1 \frac{\partial}{\partial t}(-\nabla^2)^{\frac{y}{2}-1} + \tau_2(-\nabla^2)^{\frac{y+1}{2}-1} \tag{3}$$

Here τ_1 and τ_2 are given by:

$$\tau_1 = -2\alpha_0 c_0^{y-1}, \quad \tau_2 = 2\alpha_0 c_0^y \tan\left(\frac{\pi y}{2}\right) \tag{4}$$

When the coupled first-order partial differential equations (2) are combined, the fractional Laplacian wave equation (Eq. 5) is obtained [10, 11]:

$$\frac{1}{c^2}\frac{\partial^2 p}{\partial t^2} - \nabla^2 p - \tau_1(-\nabla^2)^{\frac{y}{2}}\frac{\partial p}{\partial t} - \tau_2(-\nabla^2)^{\frac{y+1}{2}} p = S(r,t) \tag{5}$$

The numerical solution of the system of equations (2) can be efficiently computed by the CUDA version of the numerical solver software k-Wave [9, 12]. It employs the k-space pseudospectral method in which the Fourier collocation spectral method is used to compute spatial gradients and a k-space corrected finite difference scheme is used to integrate

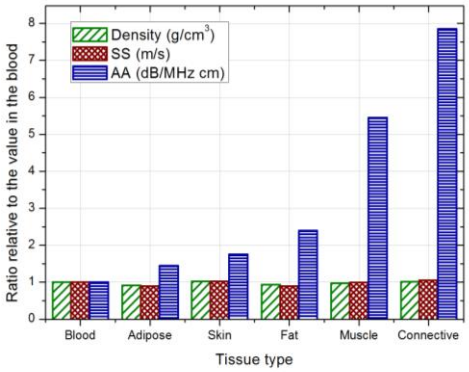

Figure 1. Comparison of density, sound speed and attenuation coefficient values relative to blood for different soft tissues [1].

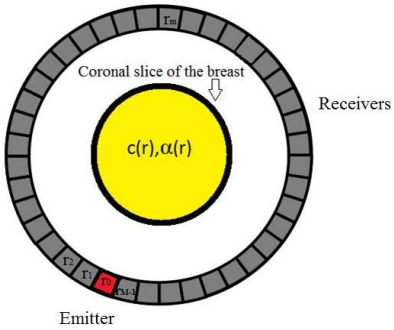

Figure 2. Scheme of an USCT system with a ring configuration conformed by M ultrasound arrays

forward in time. This scheme allows discretization close to the Nyquist limit of two grid points per minimum wavelength. This code was employed to perform the forward and backward wave propagation in our optimization algorithm and also to simulate the reference setup used to test it (schematically represented in Fig. 2).

2. INVERSION PROCEDURE

Using the set of experimental measurements of the pressure field generated by all the emitting transducers at the receiving transducers, we want to obtain the scattering potential, which represents the distribution of a certain acoustical property in the medium. Using the reconstructed potential within accurate simulations of the wave propagation, it should be possible to reproduce the set of experimental measurements of the pressure field. Norton [13] proposed a way to compute the scattering potential using an adjoint method. It is based on an iterative process which minimizes the norm of the global deviations between experimental p^{obs} and simulated signals p.

$$\varepsilon = \frac{1}{2}\sum_{m=1}^{M} \left| p(r_m) - p^{obs}(r_m) \right|^2 \tag{6}$$

In order to minimize the global error norm ε (Eq. 6) with respect to $\alpha_0(r)$, we evaluate the functional gradient $\frac{\partial \varepsilon}{\partial \alpha_0}$. This functional gradient gives the direction to update the current estimate of the scattering potential to ensure minimization of the global error.

In this work, for simplicity we only consider the effect of the attenuation due to the absorption (i.e., neglecting its effect on the dispersion, as it is relatively minor). Furthermore, as we assumed that the exponent *y* in (Eq. 1) is a constant, the inversion problem consists of recovering the distribution of the absorption coefficient α_0.

Using the adjoint method proposed in [13] and the fractional Laplacian wave equation (Eq. 5), a simple expression to calculate the functional gradient for each iteration can be obtained:

$$\frac{\partial \varepsilon}{\partial \alpha_0} = \int_0^T p^* \left[2c_0^{y-1} (-\nabla^2)^{\frac{y}{2}} \frac{\partial p}{\partial t} \right] dt \qquad (7)$$

The adjoint field (p^*) in Eq. (7) is obtained by running the wave model with an adjoint source term derived from the time-reversed difference between the experimental and simulated signals at each receiver. It is important to note that the functional gradient Eq. (7) only requires solving the wave equation Eq. (5) twice per iteration: once for the direct propagation of the pressure field generated by the emitter (to obtain p), and a second time to obtain the adjoint field (p^*).

The fractional Laplacian term in Eq. (7) becomes simpler to compute in the Fourier domain:

$$(-\nabla^2)^y p(r,t) = \mathcal{F}^{-1}\{k^{2y}\mathcal{F}[p(r,t)]\} \qquad (8)$$

Once the functional gradient is known, the distribution can be updated using a steepest descent algorithm.

$$\alpha_0{}^{it+1}(r) = \alpha_0{}^{it}(r) + \xi_k{}^{it} \frac{\partial \varepsilon}{\partial \alpha_0} \qquad (9)$$

Here $\xi_k{}^{it}$ is the step which modulates the value of the gradient in each update of the image and can be chosen by a line search method. The optimization code was implemented in C++.

3. NUMERICAL EXPERIMENTS

To test the results of the proposed algorithm, we choose to employ simulated instead of real data (to highlight the algorithmic aspects of our work and to demonstrate its feasibility to reconstruct the AA distribution). To make the numerical data more comparable to real-world experiments, random Gaussian noise was added to give a signal to noise ratio (SNR) of 40 dB, similar to the SNR present in our experimental USCT system [15] where this code will be applied in future works. The simulated setup was a circular ring of detectors of 200 point elements with a field of view of 128 mm and a 500 kHz central frequency. The simulations to obtain the reference data (or "experimental" data) were conducted with a 150 x 150 pixel grid. As the simulated noisy data was generated with the same model used for the inverse solver, the reconstruction was performed with a different sized grid of 128 x 128 pixels (to avoid inverse crime, see reference [14]). A 2-dimensional numerical phantom representing a coronal slice of breast with 4 different tissues (fat, fibroglandular tissue, benign and malignant tumors) was studied. In this work, we started the reconstruction of the attenuation with a converged map of speed of sound. The initial guess for attenuation was a homogenous map with the absorption coefficient of water (1.61 e-12 Np (rad/s)$^{-y}$ m^{-1} or 0.0022 dB (MHz)$^{-y}$ cm^{-1}) [8].

The image update using equations (7) and (9) can be obtained using the signals from one emitter and all the receivers. Nevertheless, better stability and fewer artifacts were observed when the image was updated with the average value of the functional gradients from several independent emitters. Therefore, in this work, each image update was performed with the mean functional gradient obtained by using 4 emitters. One full iteration, using the signals from all the 200 emitters, consisted of 50 image updates. The final resulting image was filtered using a median filter. To quantify the obtained results, the mean values and the standard deviation of all the pixels compounding several regions of interest (ROIs) with the same size as the lesions of the numerical phantom were obtained and compared with the expected values in those ROIs (see Fig 3 D).

4. DISCUSSION AND CONCLUSIONS

The proposed algorithm (Fig. 3A and 3B) is capable of accurately recovering the shape and values of the structures present in the real phantom. The reconstructed image was obtained in 16 minutes with 2 iterations using an Intel Xeon 16-CPU @2.4GHz with a Nvidia GeForce GTX 660. The proposed algorithm is efficient and straightforward to implement, and due to the similarity with the schemes to reconstruct the speed of sound with FWI, it will allow both acoustical distributions to be reconstructed in a common framework. These results are encouraging, and we are currently working on the reconstruction of real data. We are confident that the possibility of having quantitative US images in a reasonable time will expand the applications of this technique.

5. ACKNOWLEDGMENTS

This work was supported by Comunidad de Madrid (S2013/MIT-3024 TOPUS-CM). The authors would like to thank Jiri Jaros for assistance with the CUDA code.

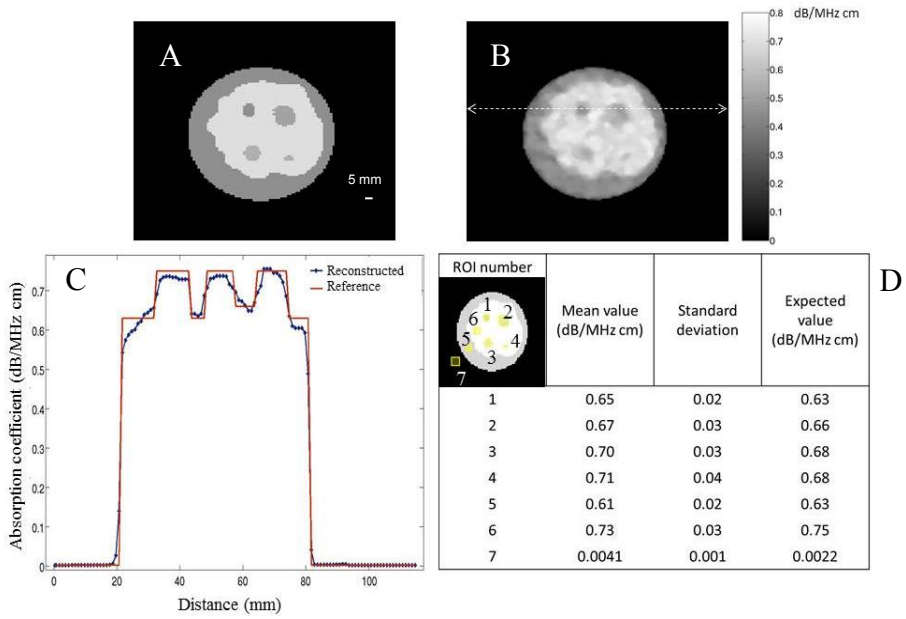

ROI number	Mean value (dB/MHz cm)	Standard deviation	Expected value (dB/MHz cm)
1	0.65	0.02	0.63
2	0.67	0.03	0.66
3	0.70	0.03	0.68
4	0.71	0.04	0.68
5	0.61	0.02	0.63
6	0.73	0.03	0.75
7	0.0041	0.001	0.0022

Figure 3. A) Numerical breast phantom. B) Reconstructed image C) Comparison of profiles D) Reconstructed values of AA against the expected ones.

6. REFERENCES

[1] T.D. Mast, "Empirical relationships between acoustic parameters in human soft tissues", *Acoustics Research Letters Online*, 1(2), pp 37-42, 2000.

[2] K. Wang, T. Matthews, F. Anis, C. Li, N. Duric and M. Anastasio, "Waveform inversion with source encoding for breast sound speed reconstruction in ultrasound computed tomography", *IEEE Transactions on Ultrasonics, Ferroelectrics, and Frequency Control*, 62(3), pp 475-493, 2015.

[3] O. Roy, I. Jovanović, A. Hormati, R. Parhizkar and M. Vetterli, "Sound speed estimation using wave-based ultrasound tomography: theory and GPU implementation", In *SPIE Medical Imaging*, p. 76290J, 2010.

[4] C. Li, G.S. Sandhu, O. Roy, N. Duric, V. Allada and S. Schmidt, "Toward a practical ultrasound waveform tomography algorithm for improving breast imaging", In *SPIE Medical Imaging*, p. 90401P, 2014.

[5] R.G. Pratt, L. Huang, N. Duric, and P. Littrup, "Sound-speed and attenuation imaging of breast tissue using waveform tomography of transmission ultrasound data", In *SPIE Medical Imaging*, p. 65104S, 2007.

[6] S. Li, M. Jackowski, D.P. Dione, T. Varslot, L.H. Staib, and K. Mueller, "Refraction corrected transmission ultrasound computed tomography for application in breast imaging", *Medical physics*, 37(5), pp 2233-2246, 2010.

[7] F. Lin, A. Nachman, and R.C. Waag, "Quantitative imaging using a time-domain eigenfunction method", *The Journal of the Acoustical Society of America*, 108(3), pp. 899-912, 2000.

[8] T.L. Szabo, Diagnostic ultrasound imaging: inside out. Elsevier Academic Press, Burlington, 2004.

[9] B.E. Treeby, and B.T. Cox, " k-Wave: MATLAB toolbox for the simulation and reconstruction of photoacoustic wave fields", *Journal of Biomedical Optics,* 15(2), p. 021314, 2010.

[10] B.E. Treeby and B.T. Cox, "Modeling power law absorption and dispersion in viscoelastic solids using a split-field and the fractional Laplacian", *The Journal of the Acoustical Society of America,* 136(4), pp 1499-1510, 2014.

[11] W. Chen and S. Holm, "Fractional Laplacian time-space models for linear and nonlinear lossy media exhibiting arbitrary frequency power-law dependency", *The Journal of the Acoustical Society of America,* 115(4), pp. 1424-1430, 2004

[12] B.E. Treeby, J. Jaros, A.P. Rendell, and B.T. Cox, "Modeling nonlinear ultrasound propagation in heterogeneous media with power law absorption using a k-space pseudospectral method", *The Journal of the Acoustical Society of America,* 131(6), pp. 4324-4336, 2012.

[13] S.J. Norton, "Iterative inverse scattering algorithms: Methods of computing Frechet derivatives", *The Journal of the Acoustical Society of America*, 106(5), pp. 2653-2660, 1999.

[14] J. Kaipio and E. Somersalo, "Statistical inverse problems: discretization, model reduction and inverse crimes", *Journal of Computational and Applied Mathematics*, 198(2), pp. 493-504, 2007.

[15] L. Medina-Valdés, M. Pérez-Liva, J. Camacho, J.M. Udías, J.L. Herraiz and N. González-Salido, "Multi-modal Ultrasound Imaging for Breast Cancer Detection", *Physics Procedia*, 63, pp. 134-140, 2015.